Acta Crystallographica Section D
Biological Crystallography
ISSN 1399-0047

Structural analysis and insight into metal-ion activation of the iron-dependent regulator from *Thermoplasma acidophilum*

Hyun Ku Yeo, Young Woo Park and Jae Young Lee*

Department of Life Science, Dongguk University Seoul, 26 Pil-dong 3-ga, Jung-gu, Seoul 100-715, Republic of Korea

Correspondence e-mail: jylee001@dongguk.edu

Received 30 December 2013
Accepted 21 February 2014

PDB references: IdeR, 4o5v; 4o6j

The iron-dependent regulator (IdeR) is a metal ion-activated transcriptional repressor that regulates the expression of genes encoding proteins involved in iron uptake to maintain metal-ion homeostasis. IdeR is a functional homologue of the diphtheria toxin repressor (DtxR), and both belong to the DtxR/MntR family of metalloregulators. The structure of Fe^{2+}-bound IdeR (TA0872) from *Themoplasma acidophilum* was determined at 2.1 Å resolution by X-ray crystallography using single-wavelength anomalous diffraction. The presence of Fe^{2+}, which is the true biological activator of IdeR, in the metal-binding site was ascertained by the use of anomalous difference electron-density maps using diffraction data collected at the Fe absorption edge. Each DtxR/IdeR subunit contains two metal ion-binding sites separated by 9 Å, labelled the primary and ancillary sites, whereas the crystal structures of IdeR from *T. acidophilum* show a binuclear iron cluster separated by 3.2 Å, which is novel to *T. acidophilum* IdeR. The metal-binding site analogous to the primary site in DtxR was unoccupied, and the ancillary site was occupied by binuclear clustered ions. This difference suggests that *T. acidophilum* IdeR and its closely related homologues are regulated by a mechanism distinct from that of either DtxR or MntR. *T. acidophilum* IdeR was also shown to have a metal-dependent DNA-binding property by electrophoretic mobility shift assay.

1. Introduction

Homeostasis of transition-metal ions is essential for living organisms. More than one-third of all proteins require metal ions for their function, which includes photosynthesis, nerve transmission and defence against toxins (Rosenzweig, 2002). Metalloregulatory proteins regulate metal-ion homeostasis in prokaryotes by binding metal ions, leading to activation or repression of the transcription of genes involved in import or export of metal ions from cells (O'Halloran, 1993). A number of metalloregulatory proteins have been identified and characterized in prokaryotes (Reyes-Caballero *et al.*, 2011). The regulation of these ions is controlled by the DtxR/MntR family to maintain Mn/Fe ion homeostasis in bacteria (Andrews *et al.*, 2003). This family is named for its founding member, the diphtheria toxin repressor (DtxR) from *Corynebacterium diphtheriae* (Boyd *et al.*, 1990; Schmitt & Holmes, 1991). This family is categorized into two subgroups: (i) the Fe^{2+}-dependent DtxR and IdeR, a homologue from *Mycobacterium tuberculosis*, and (ii) the Mn^{2+}-dependent MntR from *Bacillus subtilis* and ScaR from *Streptococcus gordonii* (Chen, Wu *et al.*, 2010). In addition to activation by Fe^{2+}, DtxR/IdeR is activated by several transition-metal ions such as Ni^{2+}, Co^{2+}, Mn^{2+}, Zn^{2+} and Cd^{2+} *in vitro* (Schmitt & Holmes,

1993; Schmitt *et al.*, 1995). However, DtxR is only activated by Fe^{2+} in its host organism, although it is responsive to either Mn^{2+} or Fe^{2+} when expressed in *B. subtilis* (Schmitt & Holmes, 1993; Guedon & Helmann, 2003). MntR is sensitive to either Mn^{2+} or Cd^{2+} *in vivo* (Que & Helmann, 2000; Guedon & Helmann, 2003). DtxR can be activated by a broad array of metal ions *in vitro*, while MntR is more selective for Cd^{2+} over Mn^{2+}, followed by Co^{2+} and Fe^{2+} and then Ni^{2+} and Zn^{2+} *in vitro* (Lieser *et al.*, 2003; Golynskiy *et al.*, 2005).

A variety of crystal structures of the DtxR/MntR family have been determined in the presence of metal ions, including Mn^{2+}, Cd^{2+}, Ca^{2+}, Ni^{2+}, Fe^{2+}, Co^{2+} and Zn^{2+} (Glasfeld *et al.*, 2003; Qiu *et al.*, 1995; Wisedchaisri *et al.*, 2007; Kliegman *et al.*, 2006; McGuire *et al.*, 2013). DtxR/IdeR orthologues consist of three domains: an N-terminal winged HTH motif DNA-binding domain (domain 1), which is composed of three α-helices and two β-strands; a dimerization domain (domain 2) with four α-helices; and a C-terminal SH3-like domain (domain 3), which is absent in Mn^{2+}-dependent MntR family proteins. DtxR/MntR family proteins contain several different metal ion-binding sites. The crystal structures of the DtxR/IdeR family have two major metal-binding sites separated by 9.0 Å. Metal-binding site 1 (the ancillary site) of *C. diphtheriae* DtxR consists of His79, Glu83 and His98 from domain 2 and Glu170 and Gln173 from domain 3, while metal-binding site 2 (the primary site) is composed of Met10 from domain 1 and Cys102, Glu105 and His106 from domain 2 (Schiering *et al.*, 1995; Pohl *et al.*, 1999). The two metal ions in the MntR family form a single binuclear cluster close to metal-binding site 2 (the primary site) and each metal ion is separated by 3.3 Å. The metal-binding site of *B. subtilis* MntR consists of Asp8 and Glu11 from domain 1 and His77, Glu99, Glu102 and His103 from domain 2, and three solvent molecules are involved in metal capture (Glasfeld *et al.*, 2003). In contrast, ScaR, an Mn^{2+}-dependent transcriptional regulator, possesses a metal-binding site that lies roughly 5 Å away from metal-binding site 1 (the ancillary site). The metal-binding site of *S. gordonii* ScaR is composed of Glu80, Cys123 and His125 from domain 2 and Asp160 from domain 3 (Stoll *et al.*, 2009).

Although the transcriptional regulation of metal-ion homeostasis in prokaryotes has been well studied, little is currently known about metal-dependent transcription regulators in archaea. MDR1 from the archaeon *Archaeoglobus fulgidus*, which is a homologue of DtxR, negatively regulates transcription in a metal-dependent manner *in vivo* and *in vitro* (Bell *et al.*, 1999). A DtxR homologue (PF0851+, genome coordinates 824684–825121) from *Pyrococcus furiosus* has been identified as a major iron-responsive transcription factor in *P. furiosus* (Zhu *et al.*, 2013). The DtxR/IdeR homologue (TA0872) from *Thermoplasma acidophilum*, which we hereafter refer to as *T. acidophilum* IdeR, has been identified and encodes a protein of 220 amino-acid residues with 27% sequence identity to DtxR from *C. diphtheriae* (Ruepp *et al.*, 2000). Further sequence comparisons of *T. acidophilum* IdeR with *M. tuberculosis* IdeR, *S. gordonii* ScaR, *B. subtilis* MntR and the *P. furiosus* DtxR homologue show 27, 26, 15 and 18%

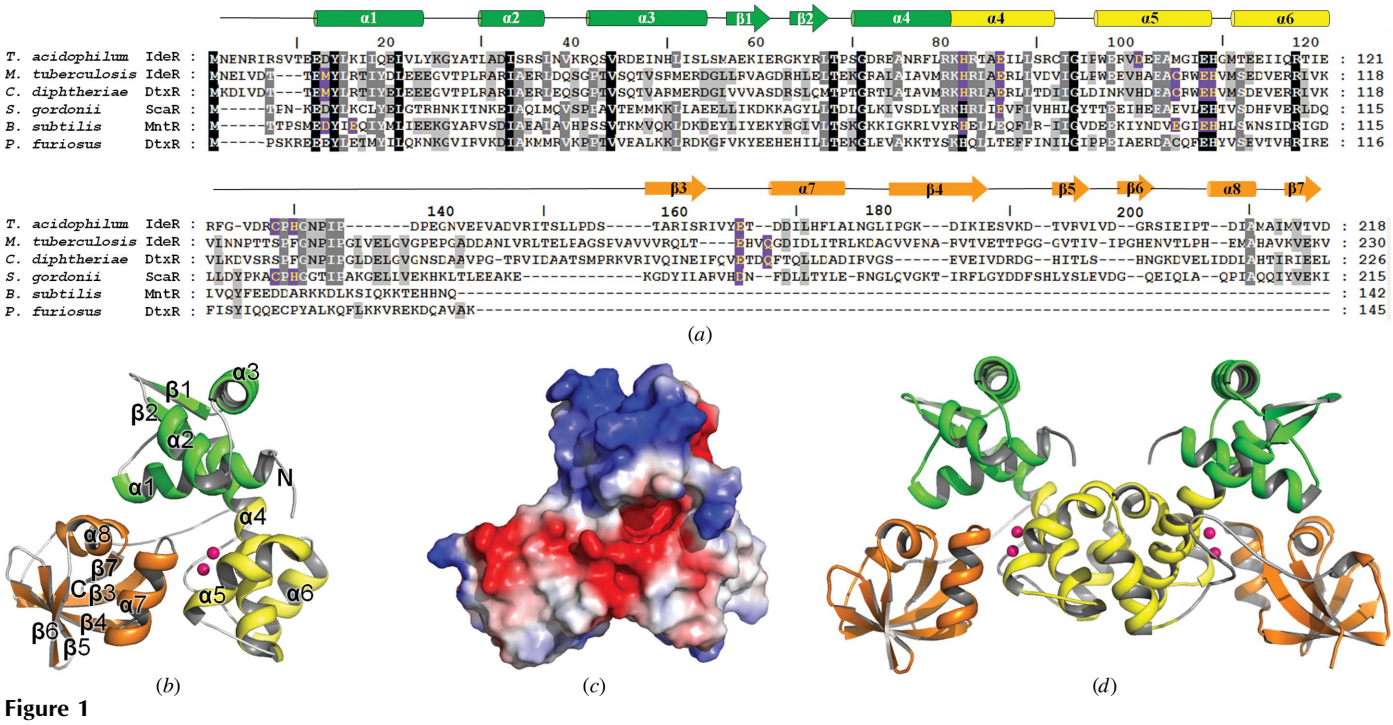

Figure 1
Structural and sequence analysis of *T. acidophilum* IdeR with the DtxR/MntR family. (*a*) Sequence alignment of *T. acidophilum* IdeR and representative DtxR/MntR family proteins. Every 20th residue is marked with a black bar above the sequence of *T. acidophilum* IdeR. Highly conserved residues and partially conserved residues are shaded in black and grey, respectively. The metal-binding residues in the DtxR/MntR structures are shaded in purple. (*b*) Overall structure of monomeric *T. acidophilum* IdeR. The domains are indicated in green, yellow and orange. (*c*) Surface electric potential representation of monomeric *T. acidophilum* IdeR; red indicates acidic charged areas and blue represents basic charged areas. (*d*) Dimeric structure of *T. acidophilum* IdeR generated by a crystallographic twofold symmetry through domain 2.

Table 1
Data-collection and refinement statistics for *T. acidophilum* IdeR.

Values in parentheses are for the highest resolution shell.

Data set	Se peak	Fe peak
Data collection		
Space group	$P2_12_12$	
Unit-cell parameters (Å, °)	a = 61.20, b = 84.97, c = 47.07, $\alpha = \beta = \gamma$ = 90	
Wavelength (Å)	0.9792	1.7394
Resolution range (Å)	50.0–2.10 (2.14–2.10)	50.0–2.30 (2.34–2.30)
Observations	103479	77121
Unique reflections	14925	11321
Completeness (%)	99.9 (100)	99.1 (97.6)
Average $I/\sigma(I)$	43.20 (13.47)	35.91 (3.36)
Multiplicity	6.9 (7.2)	6.8 (6.3)
$R_{\rm merge}$† (%)	7.5 (35.2)	7.9 (39.9)
Refinement		
Resolution (Å)	19.8–2.10 (2.17–2.10)	20.0–2.30 (2.37–2.29)
$R_{\rm cryst}/R_{\rm free}$‡ (%)	18.2/22.5 (21.9/30.4)	17.06/21.79 (22.41/23.90)
No. of protein residues	213	213
No. of metal ions	2	2
No. of solvent molecules	111	35
R.m.s.d., bonds (Å)	0.012	0.010
R.m.s.d., angles (°)	1.65	1.25
Ramachandran plot§		
Most favoured (%)	98.0	97.0
Additional allowed (%)	2.0	3.0
Generously allowed (%)	0	0
Disallowed (%)	0	0
Average B factors (Å^2)	34.00	51.40

† $R_{\rm merge} = \sum_{hkl}\sum_i |I_i(hkl) - \langle I(hkl)\rangle|/\sum_{hkl}\sum_i I_i(hkl)$, where $I(hkl)$ is the intensity of reflection hkl, $\sum_{hkl}$ is the sum over all reflections and $\sum_i$ is the sum over i measurements of reflection hkl. ‡ $R_{\rm cryst} = \sum_{hkl}||F_{\rm obs}| - |F_{\rm calc}||/\sum_{hkl}|F_{\rm obs}|$, where $R_{\rm free}$ is calculated for a randomly chosen 10% of reflections which were not used for structure refinement and $R_{\rm cryst}$ is calculated for the remaining reflections. § Determined using *MolProbity*.

sequence identity, respectively (Fig. 1*a*). Despite the determination of a number of crystal structures of the DtxR/IdeR family, structural information on Fe^{2+}-bound DtxR/IdeR has not yet been obtained. Here, we present the first crystal structure of the archaeal IdeR protein in complex with Fe^{2+}, which is the true biological activator in DtxR/IdeR. We present results of structural and biochemical studies indicating that *T. acidophilum* IdeR binds with two Fe^{2+} ions in a different fashion from the DtxR/IdeR family and may represent a new subclass of metal-dependent regulators in the DtxR/MntR family. Furthermore, an electrophoretic mobility shift assay indicates that *T. acidophilum* IdeR is capable of binding DNA in the presence of metal ions.

2. Materials and methods

2.1. Sample preparation

DNA cloning, expression and purification of *T. acidophilum* IdeR has been described previously (Yeo *et al.*, 2012). No metal ions were deliberately added during purification and crystallization. Selenomethionine (SeMet)-substituted IdeR was expressed in *Escherichia coli* BL21 Star pLysS (DE3) cells in minimal medium supplemented with 0.2% glucose, 2 µ*M* $MgSO_4$, 0.1 µ*M* $CaCl_2$ and a mixture of all amino acids at 40 mg l^{-1} except Gly, Ala, Pro, Asn, Cys and Met. When the culture reached an OD_{600} of 0.5, SeMet (50 mg l^{-1}), Phe, Thr, Lys (100 mg l^{-1}), Leu, Ile, Val and Pro (50 mg l^{-1}) were added at the same time to block Met synthesis (Van Duyne *et al.*, 1993). After 15 min, expression of recombinant protein was induced with 1 m*M* isopropyl β-D-1-thiogalactopyranoside. The cells were grown at 303 K overnight. The purification procedure for SeMet-substituted *T. acidophilum* IdeR was identical to that for the native protein except for the presence of 1 m*M* dithiothreitol in all buffers used during the purification steps.

2.2. Crystallization

The crystallization of native *T. acidophilum* IdeR has been reported previously (Yeo *et al.*, 2012). The initial crystals of SeMet-substituted IdeR were obtained by the hanging-drop vapour-diffusion method within one week by mixing equal volumes (2 µl) of the protein solution and reservoir solution at 296 K. The optimized reservoir solution consisted of 20%(*v*/*v*) PEG 4000, 0.1 *M* ammonium acetate pH 5.0, 0.35 *M* sodium acetate. The crystals were initially too small, so the microseeding technique was used to grow larger crystals. A stock solution of microseeds was prepared by crushing 50–100 microcrystals in 0.10 ml reservoir solution and serially diluting the suspension by a factor of 100. Each hanging drop was prepared by mixing the protein solution, the reservoir solution and the microseed solution in a ratio of 1:1:0.1. Crystals grew reproducibly up to a maximum size of approximately 0.2 × 0.2 × 0.05 mm within one week. Fe^{2+} ions were not intentionally added during the crystallization step. Iron was apparently picked up by the recombinant protein in *E. coli* and remained bound to the protein throughout the purification and crystallization steps.

2.3. Data collection

A crystal of the SeMet-substituted protein was transferred into a cryoprotectant consisting of 20%(*v*/*v*) glycerol in the reservoir solution. Single-wavelength anomalous diffraction (SAD) data were collected to 2.1 Å resolution at 100 K using an ADSC Quantum 315 CCD image-plate detector on beamline 5C of the Pohang Accelerator Laboratory, Republic of Korea. The data were collected at a wavelength of 0.9792 Å using a 1° oscillation per image with a crystal-to-detector distance of 250 mm. The crystals belonged to the orthorhombic space group $P2_12_12$, with unit-cell parameters a = 61.20, b = 84.97, c = 47.07 Å, $\alpha = \beta = \gamma = 90°$. One IdeR monomer was present in the asymmetric unit, giving a solvent fraction of 44.6%. Following positive identification of Fe^{2+} ions in the crystals by X-ray fluorescence, complete data were collected to 2.3 Å resolution at the Fe edge (λ = 1.7394 Å) using an ADSC Quantum 210 CCD image-plate detector on beamline 7A of the Pohang Accelerator Laboratory, Republic of Korea. All data were processed and scaled using *DENZO* and *SCALEPACK* from the *HKL*-2000 program suite (Otwinowski & Minor, 1997).

2.4. Structure determination and refinement

Selenium-site searching was performed and the SAD-phased electron-density map was interpreted using *AutoSol*

from *PHENIX* to build an initial model which accounted for approximately 25% of the residues (Adams *et al.*, 2010). Subsequently, the model was built manually using *Coot* (Emsley *et al.*, 2010). The model of SeMet-labelled IdeR was refined with *REFMAC* in the *CCP*4 program suite (Murshudov *et al.*, 2011; Winn *et al.*, 2011), including bulk-solvent correction, and the *PHENIX* program package (Adams *et al.*, 2010). The refined model of Fe^{2+}-bound SeMet-labelled IdeR, accounting for 213 residues in one IdeR monomer, 113 water molecules and two Fe^{2+} ions in the asymmetric unit, gave R_{work} and R_{free} values of 18.2 and 22.5%, respectively, for data in the resolution range 19.8–2.10 Å (Table 1). A random set of 5% of the reflections was excluded from the refinement for cross-validation of the refinement strategy. The quality of the model was checked using *MolProbity* (Chen, Arendall *et al.*, 2010). All residues were in the favoured region of the Ramachandran plot. The X-ray data-collection and refinement statistics are presented in Table 1. The coordinates and structure factors have been deposited in the Protein Data Bank as entries 4o5v and 4o6j for SeMet-labelled IdeR and native IdeR at the Fe peak wavelength, respectively.

2.5. Electrophoretic mobility shift assay

To assess the DNA-binding ability of the purified IdeR from *T. acidophilum*, a 300 bp DNA containing its own promoter region was prepared by polymerase chain reaction using the primers Ta300F (5′-GGAAATTCCATATGGAGAATACT-GCTTCAGTTATCTC-3′) and Ta300R (5′-CGGCTCGAG-ATTATCTTTAGGTAGTCCTCT-3′). The reaction buffer consisted of 50 m*M* Tris pH 7.5, 100 m*M* NaCl, 5 m*M* $MgCl_2$, 10% glycerol, 0.2% bovine serum albumin. The *T. acidophilum* IdeR proteins (final concentration 5.0 µ*M*) were added to the reaction mixture prior to the 300 bp DNA. Metal ions or 5 m*M* EDTA were also added to the reaction mixture. All binding reactions were performed in a total volume of 20 µl on ice for 30 min. For EMSA, 10× stock solutions were freshly prepared using $FeSO_4.7H_2O$, $MnCl_2.4H_2O$, $ZnSO_4.7H_2O$, $CoCl_2.6H_2O$ (Sigma) or $Na_2EDTA.2H_2O$ (Biopure). The incubated mixture was resolved on a 6% pre-chilled non-denaturing polyacrylamide gel in Tris–glycine buffer (no EDTA) pH 8.8 at 50 V. After electrophoresis at 4°C, the gel was visualized using an EMSA staining kit (Life Technology).

2.6. Iron-chelating assay

Ferrous ion was detected using the phenanthroline assay (Tamura *et al.*, 1974) with slight modifications. 20 µl 500 µ*M* IdeR was mixed with 30 µl distilled water and heated for 15 min at 100°C. After centrifugation at 13 000*g* for 2 min, 20 µl supernatant was added to a mixture of gel buffer and 20 µl 1,10-phenanthroline to make 100 µl samples. The samples were mixed thoroughly after every addition. The control reaction consisted of a mixture of gel buffer (20 m*M* Tris pH 8.0, 5% glycerol, 5 m*M* $MgCl_2$, 100 m*M* NaCl, 1 m*M* DTT) and 0.1%(*w*/*v*) 1,10-phenanthroline. To compare the concentration of ferrous ion in *T. acidophilum* IdeR, the same amounts of $FeSO_4$ and $FeCl_3$ were calculated using the same protocol. Reactions were incubated for 1 h at room temperature and the absorbance was measured at 510 nm. In order to measure the composition of Fe^{2+} and Fe^{3+}, Fe^{3+} was reduced to Fe^{2+} using an excess of ascorbic acid. Ascorbic acid showed the maximum capacity as a reducing agent of Fe^{3+} (Elmagirbi *et al.*, 2012). To determine the Fe^{2+} concentration alone, the assay was performed without ascorbic acid. The absorbance and iron-composition data are shown in Supplementary Table S1[1]. To calculate the number of moles of iron bound to *T. acidophilum* IdeR, a molar extinction coefficient of 11 100 mol^{-1} cm^{-1} for 1,10-phenanthroline was used.

3. Results and discussion

3.1. Overall structure of *T. acidophilum* IdeR

The crystal structure of *T. acidophilum* IdeR was determined at 2.1 Å resolution using SAD data sets collected at the selenium peak (0.9792 Å). The structure was refined to crystallographic R_{work} and R_{free} values of 18.2 and 22.5%, respectively, with good geometry. The refined model (PDB entry 4o5v) contained 213 amino-acid residues of the monomer in the asymmetric unit and was assessed using *MolProbity* (Chen, Arendall *et al.*, 2010). Seven residues (Met1–Arg5 and Asp219–Arg220) were disordered in the crystal and are not visible in the electron-density map. Two Fe^{2+} ions were bound to each *T. acidophilum* IdeR monomer. Iron was quantified at 1.0 mol iron per mole of IdeR monomer by a chelation assay; the estimation of reduced iron in the protein preparations is somewhat uncertain, but may be as high as 80% (Supplementary Table S1). In this current structure, there is no sign of oxidative modification of cysteine residues (Cys92 and Cys128). Cys92 formed a disulfide bond to Cys92 from the other subunit, while Cys128 makes a direct coordination to the metal atom. Each subunit consisted of eight helices and seven strands and was divided into three domains: an N-terminal DNA-binding domain (domain 1; residues 11–76), a dimerization domain (domain 2; residues 77–124) and a C-terminal domain (domain 3; residues 149–218). The overall structure of *T. acidophilum* IdeR is shown in Fig. 1(*b*). Domain 1 contained three α-helices and a pair of antiparallel β-strands. Helices α2 and α3 and their intervening loop, together with the β-strands, form a winged helix–turn–helix (HTH) motif, which is a putative DNA-binding region (Brennan & Matthews, 1989). Even though there were some variations in the angles or lengths of the HTH motif helices, helix α3 of the HTH motif was responsible for DNA recognition by base-specific DNA interactions. Thus, we speculated that positively charged residues (Lys39, Arg40 and Arg45) in *T. acidophilum* IdeR helix α3 are involved in DNA binding. Domain 2, the dimerization domain, was composed of three α-helices (α4–α6). Domains 1 and 2 are connected by a long linker helix α4 (residues 69–93). Although a monomer of *T. acidophilum* IdeR is present in each asymmetric unit of the

[1] Supporting information has been deposited in the IUCr electronic archive (Reference: MH5126).

crystal, it forms a dimeric unit, with approximate dimensions of 100 × 50 × 40 Å, by the association of two monomers related by crystallographic twofold symmetry through their dimerization domains (Fig. 1*d*). The solvent-accessible surface area buried at the interface between the two monomers in this dimeric unit was ∼800 Å^2 (∼7.3% of the monomer surface area), and 20 amino-acid residues were involved in this interface (*PDBePISA* protein–protein interaction server; http://www.ebi.ac.uk/msd-srv/prot_int/). The dimer interface is mainly contributed by hydrophobic side chains such as Leu88, Leu89, Ile93, Ile95, Pro96, Gly106, Ile107, Gly110, Met111, Ile115, Thr11 and Phe123. Six hydrogen bonds were formed between Cys92 O and Arg122 N$^{\varepsilon}$, between Gly94 O and Arg118 NH1 and between Glu103 O$^{\varepsilon1}$ and Thr112 O$^{\gamma1}$. Cys92 formed a disulfide bond to Cys92 from the other subunit with a distance of 2.14 Å. This finding raises the possibility that *T. acidophilum* IdeR may exist as a functional dimer in solution.

3.2. Structural comparison with other proteins

We carried out a search to identify structurally similar proteins using the *DALI* server (Holm & Sander, 1993). The best three matches belonged to the metal-dependent DtxR/MntR family. They were (i) the iron-dependent repressor IdeR from *M. tuberculosis* (Feese *et al.*, 2001; PDB entry 1fx7; r.m.s. deviation of 2.9 Å for 210 equivalent C$^{\alpha}$ positions in residues 6–218 of *T. acidophilum* IdeR, *Z*-score of 23.5 and sequence identity of 27%), (ii) *C. diphtheriae* DtxR in complex with DNA (Pohl *et al.*, 1999; PDB entry 1c0w; r.m.s. deviation of 3.2 Å for 206 equivalent C$^{\alpha}$ positions in residues 6–218 of *T. acidophilum* IdeR, *Z*-score of 22.2 and sequence identity of 26%) and (iii) *S. gordonii* ScaR in complex with DNA (Stoll *et al.*, 2009; PDB entry 3hru; r.m.s. deviation of 2.8 Å for 207 equivalent C$^{\alpha}$ positions in residues 6–213 of *T. acidophilum* IdeR, *Z*-score of 21.1 and sequence identity of 27%).

We further elaborated the structural similarity search with individual domains of the *T. acidophilum* IdeR. The result using domains 1 and 2 (residues 6–125) is similar to that obtained using the whole structure of *T. acidophilum* IdeR. The highest structural similarity was obtained with the *C. diphtheriae* DtxR mutant (C102D) in complex with DNA (Chen *et al.*, 2000; PDB entry 1f5t; r.m.s deviation of 2.2 Å for 119 equivalent C$^{\alpha}$ positions in residues 6–125 of *T. acidophilum* IdeR, *Z*-score of 16.5 and sequence identity of 28%). The second highest similarity was found with *M. tuberculosis* IdeR (Feese *et al.*, 2001; PDB entry 1fx7; r.m.s. deviation of 1.9 Å for 120 equivalent C$^{\alpha}$ positions in residues 6–125 of

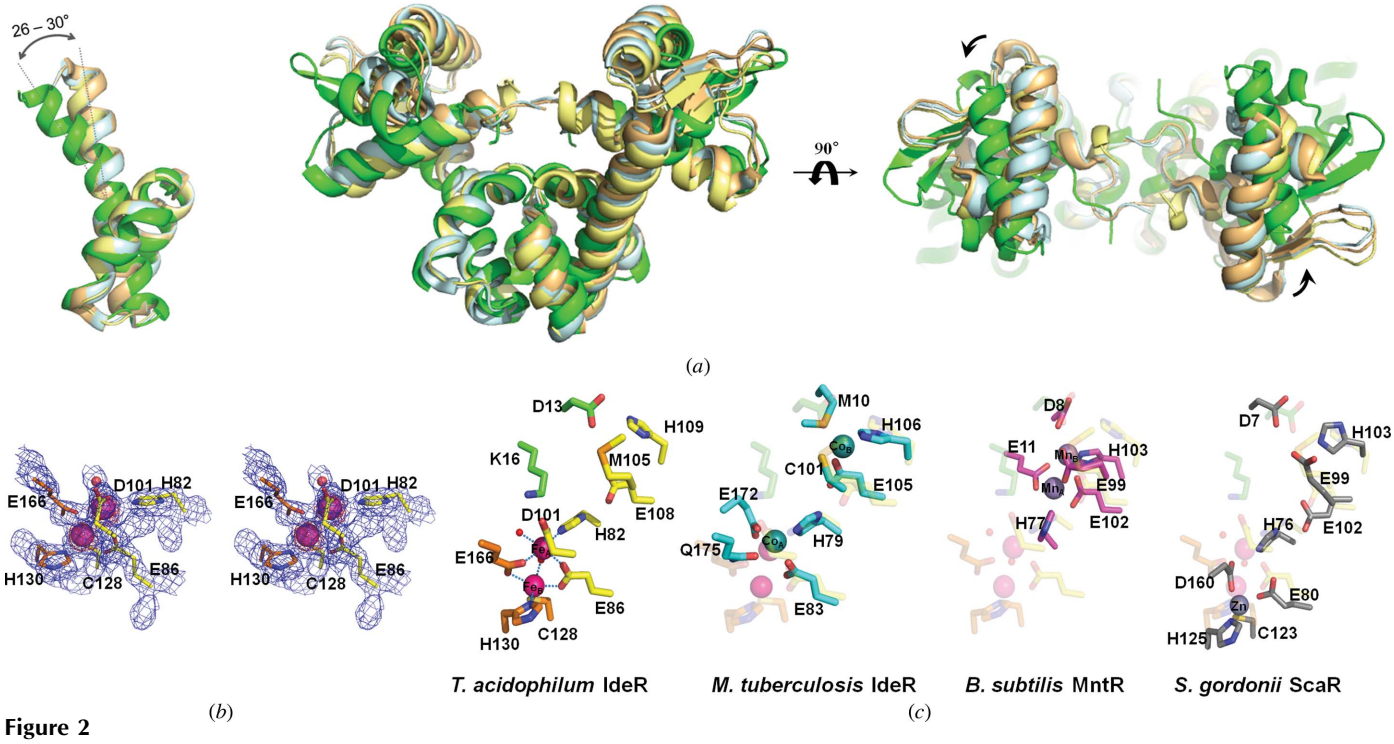

Figure 2
Structural comparison and metal ion-binding site in *T. acidophilum* IdeR. (*a*) Two views of structural superposition between *T. acidophilum* IdeR and the DtxR/MntR family proteins, aligned by the dimerization domain of one subunit. The SH3-like domains (domain 3) are omitted for clarity. The left image is obtained by additional elimination of the DNA-binding domains of these structures. The *T. acidophilum* IdeR structure is shown in green. *C. diphtheriae* apo DtxR (PDB entry 1bi2), *M. tuberculosis* IdeR (PDB entry 1fx7) and the *M. tuberculosis* IdeR–DNA complex (PDB entry 1u8r) structures are shown in light cyan, light yellow and light orange, respectively. (*b*) Stereoview of the metal-binding site in *T. acidophilum* IdeR. A σ_A-weighted electron-density map ($2F_o - F_c$ map) contoured at 1.6σ (blue). The anomalous difference map contoured at 8σ (red) was calculated using Bijovet differences collected at the ferrous peak wavelength (1.7394 Å). The Fe^{2+} ions (magenta) are depicted with surrounding residues (yellow sticks from domain 2 and orange sticks from domain 3) and waters (red). (*c*) Various metal-binding sites in the DtxR/MntR family. The Fe^{2+} ion cluster in *T. acidophilum* IdeR, two metal-binding sites (ancillary and primary) in *M. tuberculosis* IdeR, the Mn^{2+}-binding cluster in *B. subtilis* MntR and one Zn^{2+}-binding site in *S. gordonii* ScaR are shown as stick models. The Fe^{2+} ion cluster in *T. acidophilum* IdeR is aligned in transparent mode. The participating metal-binding residues are indicated. Fe^{2+}, Co^{2+}, Mn^{2+} and Zn^{2+} ions are indicated in magenta, cyan, purple and grey, respectively.

T. acidophilum IdeR, *Z*-score of 23.3 and sequence identity of 29%). Using domain 3 (residues 146–218) alone, the highest *Z*-score was obtained with the *Thermococcus thioreducens* ferrous ion-transport protein (FeoA; R. C. Hughes, Y. Li, B.-C. Wang, Z.-J. Liu & J. D. Ng, unpublished work; PDB entry 3e19; r.m.s deviation of 1.3 Å for 72 equivalent C^{α} positions in residues 146–218 of *T. acidophilum* IdeR, *Z*-score of 13.4 and sequence identity of 21%) and the next highest similarity was found with the FeoA domain of the *S. gordonii* ScaR protein (Stoll *et al.*, 2009; PDB entry 3hru; r.m.s. deviation of 1.5 Å for 72 equivalent C^{α} positions in residues 146–218 of *T. acidophilum* IdeR, *Z*-score of 12.6 and sequence identity of 25%). The observed structural and sequence similarity of *T. acidophilum* IdeR to other DtxR/IdeR family proteins implies functional relatedness.

Previous studies revealed that *C. diphtheriae* DtxR changes conformation when it binds to the target DNA by inducing a hinge-bending motion at about residue 74 (Qiu *et al.*, 1995; Pohl *et al.*, 1998). To investigate the hinge-motion properties of *T. acidophilum* IdeR, we compared the domain orientation by superimposing the C^{α} atoms of domain 2 (77–124) of the *T. acidophilum* IdeR structure with apo DtxR (Pohl *et al.*, 1998), Co^{2+}-IdeR from *M. tuberculosis* (Feese *et al.*, 2001) and the Co^{2+}-IdeR–DNA complex structure (Wisedchaisri *et al.*, 2007). The r.m.s deviations in C^{α} positions for domain 2 (residues 77–124) are 1.24, 1.14 and 1.18 Å, respectively. When the dimerization domain is superimposed, the DNA-binding domains vary by 3.7–5.1 Å (at residue Asp46). The movement of the DNA-binding domain with respect to domain 2 is centred at residue Leu79 of helix α4 and is kinked by 26–30° (Fig. 2*a*). There is a loss of hydrogen bonding within helix α4 between Arg77 O and Lys81 N, with a distance of 3.9 Å. This reorientation is considerably larger than the motion observed in the crystal structures of *C. diphtheriae* DtxR and *M. tuberculosis* IdeR, where the same angle is only ∼2.0°. The separation between the DNA-binding domains of the *T. acidophilum* IdeR dimer is slightly larger than that observed in those of *C. diphtheriae* DtxR or *M. tuberculosis* IdeR. When measured between the C^{α} atoms of Asp46, at the centre of the recognition helix, the domain separation is 33 Å in *T. acidophilum* IdeR, while the separations between comparable positions are 28, 27 and 28 Å for apo DtxR, Co^{2+}-IdeR and the Co^{2+}-IdeR–DNA complex, respectively (Supplementary Table S2).

3.3. Metal-binding site

The Fe^{2+} ions at metal-binding sites were identified in an $F_{obs} - F_{calc}$ difference electron-density map, which showed two peaks even at a 10σ contour level. The presence of Fe^{2+} ions in *T. acidophilum* IdeR was ascertained by constructing an anomalous difference electron-density map (Fig. 2*a*) using diffraction data at the Fe edge (Table 1). The metal-binding sites appeared to be fully occupied, with temperature factors for the two Fe^{2+} ions of 15.17 and 15.50 $Å^2$, respectively. Strikingly, our crystal structure of *T. acidophilum* IdeR revealed that the two Fe^{2+} ions formed a binuclear iron cluster with one Fe^{2+} ion (Fe_A) bound in an octahedral coordination

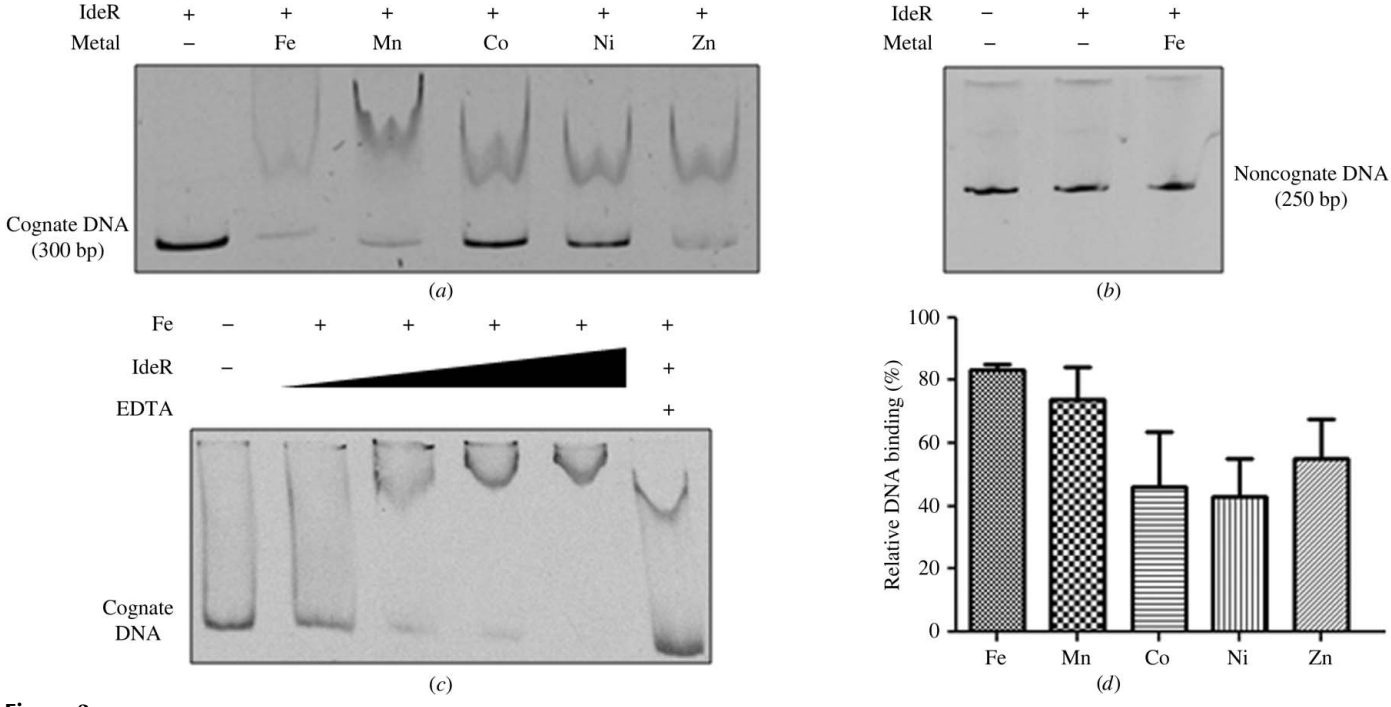

Figure 3
Electrophoretic mobility shift assay of *T. acidophilum* IdeR. (*a*) EMSA was performed using a 300 bp DNA containing base pairs −250 to +50 relative to the start site of the *T. acidophilum* IdeR transcript (TA0872) with various metal ions. (*b*) Noncognate 250 bp DNA was used as a negative control. (*c*) 10 n*M* dsDNA was incubated on ice for 30 min in the presence of Fe^{2+} ions. All lanes contained 10 n*M* dsDNA; lane 1, no protein; lanes 2–5, 0.25, 0.5, 1 and 2 µ*M* *T. acidophilum* IdeR; lane 6, treated with 5 m*M* EDTA after incubation. (*d*) Relative DNA-binding activities of *T. acidophilum* IdeR were measured with various metal ions. Data represent mean relative DNA-binding acitivities with standard error of three independent measurements.

and the other Fe^{2+} ion (Fe_B) bound in a trigonal pyramidal coordination environment and separated by 3.2 Å. The binuclear Fe^{2+} ions were liganded by six protein side chains: His82, Glu86, Asp101, Cys128 and His130 contributed by domain 2 and Glu166 contributed by domain 3 (Fig. 2*b*). The two Fe^{2+} ions (Fe_A and Fe_B) were jointly coordinated by the carboxylate O atoms of Glu86 from domain 2 and Glu166 from domain 3 and by a water molecule (Fig. 2*b*). In addition, the metal ions were individually coordinated by His82 (Fe_A), Asp101 (Fe_A), Cys128 (Fe_B) and His130 (Fe_B). The Fe_A ion was also coordinated by an additional water molecule in a near-perfect octahedral geometry. Furthermore, there is no sixth ligand in the Fe_B ion coordinated with distorted trigonal pyramidal geometry. The Fe_A site is analogous to metal-binding site 1 (the ancillary site) in DtxR, while the Fe_B site is analogous to the secondary site in ScaR.

Based on sequence alignments, metal-binding site 2 (the primary site) formed by Met10, Cys102, Glu105 and His106 in DtxR would be conserved in *T. acidophilum* IdeR. In *T. acidophilum* IdeR, the corresponding residues are Asp13, Met105, Glu108 and His109. Met10 and Cys102 in *C. diphtheriae* DtxR, corresponding to Asp13 and Met105 in *T. acidophilum* IdeR, have been reported to be responsible for metal selectivity in the *C. diphtheriae* protein (Guedon & Helmann, 2003; Glasfeld *et al.*, 2003). No metal binding is observed to this site in any of the structures reported here, although the residues are positioned appropriately to form a binding site. The reason for the lack of bound metal at this putative site is unclear. It is possibly partly owing to the low pH (5.0) of crystallization or the high concentration (∼0.5 *M*) of Na^+ ions during crystallization process. It will be valuable to verify the metal binding at metal-binding site 2 (primary site) in future experiments.

3.4. DNA binding of IdeR

The complete genome sequence of *T. acidophilum* (Ruepp *et al.*, 2000) contains an IdeR-like gene (TA0872) which is homologous to that for *C. diphtheriae* DtxR (Boyd *et al.*, 1990; Tao *et al.*, 1994). The DtxR family proteins bind DNA in the presence of metal ions (Guedon & Helmann, 2003). The true biological activator is Fe^{2+}, although DtxR/IdeR is activated by other transition-metal ions *in vitro*, including Mn^{2+}, Co^{2+}, Ni^{2+}, Zn^{2+} and Cd^{2+} (Tao & Murphy, 1992). In the *T. acidophilum* genome, an operon-like structure including *T. acidophilum* IdeR (TA0872) was identified upstream of four genes homologous to a membrane protein (TA0870), an ABC-transporter protein (TA0869) and two hypothetical proteins (TA0871 and TA0868). Therefore, we speculate that *T. acidophilum* IdeR binds to its own promoter and regulates the transcription of this operon in a metal-dependent manner.

To determine whether *T. acidophilum* IdeR binds to DNA, we performed electrophoretic mobility shift assays using a 300 bp DNA containing base pairs −250 to +50 relative to the start site of the *T. acidophilum* IdeR transcript (TA0872) with various metal ions. We found that the DNA band was shifted in the presence of IdeR and Fe^{2+} in a protein dose-dependent manner (Fig. 3*b*). As a control, bovine serum albumin did not bind the same DNA (Fig. 3*b*). When residual metal ions bound to IdeR were removed by excess EDTA, the binding ability of IdeR was much reduced (Fig. 3*a*). This result clearly indicates that the shift of the DNA band was owing to binding of IdeR in complex with Fe^{2+}. To assess the role of other divalent metal ions in DNA binding, we conducted the assay in the presence of various metal ions. Strong DNA binding by IdeR was observed in the presence of Fe^{2+}, Mn^{2+} and Zn^{2+}. In contrast, relatively weak DNA binding was observed in the presence of Co^{2+} and Ni^{2+} (Fig. 3*d*). Furthermore, significant complex formation was not observed with a noncognate 250 bp DNA (Fig. 3*b*). This result demonstrates that *T. acidophilum* IdeR binds to its own promoter in a metal-dependent manner *in vitro*.

4. Conclusion

We determined the structure of the archaeal *T. acidophilum* IdeR in complex with Fe^{2+} ions. Our results show that *T. acidophilum* IdeR consists of three domains. The two Fe^{2+} ions form a binuclear iron cluster in the metal-binding site of *T. acidophilum* IdeR *via* six amino-acid residues: three strictly conserved residues (His82, Glu86 and Asp101) in the DtxR/MntR family, two residues (Cys128 and His130) that are conserved in ScaR, and Glu166 conserved in the DtxR/IdeR family (Figs. 1*a* and 2*b*). The unique feature of this binuclear iron cluster suggests that *T. acidophilum* IdeR and its closely related homologues could be regulated by a mechanism distinct from that of either DtxR or MntR and may represent a new subclass of metal-dependent regulators in the DtxR/MntR family (Fig. 2*b*). We also showed that *T. acidophilum* IdeR binds its own promoter region in the presence of a variety of metal ions *in vitro*. Although the assignment of a functional role for *T. acidophilum* IdeR is tentative, these data suggest that *T. acidophilum* IdeR may function as an iron-dependent transcriptional regulator, supporting the previous assignment of *T. acidophilum* IdeR as a member of the DtxR/MntR family based on primary sequence.

We thank the staff members at Pohang Accelerator Laboratory beamlines 7A and 5C for their help with data collection. HKY is a recipient of the Global PhD Fellowship program (NRF-2011-0031110). This work was supported by the National Research Foundation of Korea (NRF-2011-0014251) and the Agriculture Research Center (ARC, 710003-03) program of the Ministry for Food, Agriculture, Forestry and Fisheries, Republic of Korea. The authors declare no competing commercial interests related to this work.

References

Adams, P. D. *et al.* (2010). *Acta Cryst.* D**66**, 213–221.
Andrews, S. C., Robinson, A. K. & Rodríguez-Quiñones, F. (2003). *FEMS Microbiol. Rev.* **27**, 215–237.
Bell, S. D., Cairns, S. S., Robson, R. L. & Jackson, S. P. (1999). *Mol. Cell*, **4**, 971–982.
Boyd, J., Oza, M. N. & Murphy, J. R. (1990). *Proc. Natl Acad. Sci. USA*, **87**, 5968–5972.

Brennan, R. G. & Matthews, B. W. (1989). *J. Biol. Chem.* **264**, 1903–1906.
Chen, C. S., White, A., Love, J., Murphy, J. R. & Ringe, D. (2000). *Biochemistry*, **39**, 10397–10407.
Chen, H., Wu, R., Xu, G., Fang, X., Qiu, X., Guo, H., Tian, B. & Hua, Y. (2010). *Biochem. Biophys. Res. Commun.* **396**, 413–418.
Chen, V. B., Arendall, W. B., Headd, J. J., Keedy, D. A., Immormino, R. M., Kapral, G. J., Murray, L. W., Richardson, J. S. & Richardson, D. C. (2010). *Acta Cryst.* D**66**, 12–21.
Elmagirbi, A., Sulistyaarti, H. & Atikah, A. (2012). *J. Pure Appl. Chem. Res.* **1**, 11–17.
Emsley, P., Lohkamp, B., Scott, W. G. & Cowtan, K. (2010). *Acta Cryst.* D**66**, 486–501.
Feese, M. D., Ingason, B. P., Goranson-Siekierke, J., Holmes, R. K. & Hol, W. G. (2001). *J. Biol. Chem.* **276**, 5959–5966.
Glasfeld, A., Guedon, E., Helmann, J. D. & Brennan, R. G. (2003). *Nature Struct. Biol.* **10**, 652–657.
Golynskiy, M. V., Davis, T. C., Helmann, J. D. & Cohen, S. M. (2005). *Biochemistry*, **44**, 3380–3389.
Guedon, E. & Helmann, J. D. (2003). *Mol. Microbiol.* **48**, 495–506.
Holm, L. & Sander, C. (1993). *J. Mol. Biol.* **233**, 123–138.
Kliegman, J. I., Griner, S. L., Helmann, J. D., Brennan, R. G. & Glasfeld, A. (2006). *Biochemistry*, **45**, 3493–3505.
Lieser, S. A., Davis, T. C., Helmann, J. D. & Cohen, S. M. (2003). *Biochemistry*, **42**, 12634–12642.
McGuire, A. M., Cuthbert, B. J., Ma, Z., Grauer-Gray, K. D., Brunjes Brophy, M., Spear, K. A., Soonsanga, S., Kliegman, J. I., Griner, S. L., Helmann, J. D. & Glasfeld, A. (2013). *Biochemistry*, **52**, 701–713.
Murshudov, G. N., Skubák, P., Lebedev, A. A., Pannu, N. S., Steiner, R. A., Nicholls, R. A., Winn, M. D., Long, F. & Vagin, A. A. (2011). *Acta Cryst.* D**67**, 355–367.
O'Halloran, T. V. (1993). *Science*, **261**, 715–725.
Otwinowski, Z. & Minor, W. (1997). *Methods Enzymol.* **276**, 307–326.
Pohl, E., Holmes, R. K. & Hol, W. G. J. (1998). *J. Biol. Chem.* **273**, 22420–22427.
Pohl, E., Holmes, R. K. & Hol, W. G. J. (1999). *J. Mol. Biol.* **292**, 653–667.
Qiu, X., Verlinde, C. L., Zhang, S., Schmitt, M. P., Holmes, R. K. & Hol, W. G. J. (1995). *Structure*, **3**, 87–100.
Que, Q. & Helmann, J. D. (2000). *Mol. Microbiol.* **35**, 1454–1468.
Reyes-Caballero, H., Campanello, G. C. & Giedroc, D. P. (2011). *Biophys. Chem.* **156**, 103–114.
Rosenzweig, A. C. (2002). *Chem. Biol.* **9**, 673–677.
Ruepp, A., Graml, W., Santos-Martinez, M. L., Koretke, K. K., Volker, C., Mewes, H. W., Frishman, D., Stocker, S., Lupas, A. N. & Baumeister, W. (2000). *Nature (London)*, **407**, 508–513.
Schiering, N., Tao, X., Zeng, H., Murphy, J. R., Petsko, G. A. & Ringe, D. (1995). *Proc. Natl Acad. Sci. USA*, **92**, 9843–9850.
Schmitt, M. P. & Holmes, R. K. (1991). *Infect. Immun.* **59**, 3903–3908.
Schmitt, M. P. & Holmes, R. K. (1993). *Mol. Microbiol.* **9**, 173–181.
Schmitt, M. P., Predich, M., Doukhan, L., Smith, I. & Holmes, R. K. (1995). *Infect. Immun.* **63**, 4284–4289.
Stoll, K. E., Draper, W. E., Kliegman, J. I., Golynskiy, M. V., Brew-Appiah, R. A., Phillips, R. K., Brown, H. K., Breyer, W. A., Jakubovics, N. S., Jenkinson, H. F., Brennan, R. G., Cohen, S. M. & Glasfeld, A. (2009). *Biochemistry*, **48**, 10308–10320.
Tamura, H., Goto, K., Yotsuyanagi, T. & Nagayama, M. (1974). *Talanta*, **21**, 314–318.
Tao, X. & Murphy, J. R. (1992). *J. Biol. Chem.* **267**, 21761–21764.
Tao, X., Schiering, N., Zeng, H., Ringe, D. & Murphy, J. R. (1994). *Mol. Microbiol.* **14**, 191–197.
Van Duyne, G. D., Standaert, R. F., Karplus, P. A., Schreiber, S. L. & Clardy, J. (1993). *J. Mol. Biol.* **229**, 105–124.
Winn, M. D. *et al.* (2011). *Acta Cryst.* D**67**, 235–242.
Wisedchaisri, G., Chou, C. J., Wu, M., Roach, C., Rice, A. E., Holmes, R. K., Beeson, C. & Hol, W. G. J. (2007). *Biochemistry*, **46**, 436–447.
Yeo, H. K., Kang, J., Park, Y. W., Sung, J.-S. & Lee, J. Y. (2012). *Acta Cryst.* F**68**, 172–174.
Zhu, Y., Kumar, S., Menon, A. L., Scott, R. A. & Adams, M. W. W. (2013). *J. Bacteriol.* **195**, 2400–2407.